MOLECULAR AND CELLULAR BIOLOGY, Jan. 2000, p. 299–311 Vol. 20, No. 1
0270-7306/00/$04.00+0

Activated Mutants of SHP-2 Preferentially Induce Elongation of *Xenopus* Animal Caps

ALANA M. O'REILLY,[1] SCOTT PLUSKEY,[2] STEVEN E. SHOELSON,[2] AND BENJAMIN G. NEEL[1]*

Cancer Biology Program, Division of Hematology-Oncology, Department of Medicine, Beth Israel-Deaconess Medical Center and Harvard Medical School,[1] and Joslin Diabetes Center and Department of Medicine, Brigham and Women's Hospital, Harvard Medical School,[2] Boston, Massachusetts

Received 12 July 1999/Returned for modification 9 August 1999/Accepted 1 September 1999

In *Xenopus* ectodermal explants (animal caps), fibroblast growth factor (FGF) evokes two major events: induction of ventrolateral mesodermal tissues and elongation. The *Xenopus* FGF receptor (XFGFR) and certain downstream components of the XFGFR signal transduction pathway (e.g., members of the Ras/Raf/MEK/mitogen-activated protein kinase [MAPK] cascade) are required for both of these processes. Likewise, activated versions of these signaling components induce mesoderm and promote animal cap elongation. Previously, using a dominant negative mutant approach, we showed that the protein-tyrosine phosphatase SHP-2 is necessary for FGF-induced MAPK activation, mesoderm induction, and elongation of animal caps. Taking advantage of recent structural information, we now have generated novel, activated mutants of SHP-2. Here, we show that expression of these mutants induces animal cap elongation to an extent comparable to that evoked by FGF. Surprisingly, however, activated mutant-induced elongation can occur without mesodermal cytodifferentiation and is accompanied by minimal activation of the MAPK pathway and mesodermal marker expression. Our results implicate SHP-2 in a pathway(s) directing cell movements in vivo and identify potential downstream components of this pathway. Our activated mutants also may be useful for determining the specific functions of SHP-2 in other signaling systems.

Growth factor-mediated signal transduction is a well-recognized mechanism for controlling cell growth, differentiation, and movement. Orchestration of these processes is essential for complex events such as embryonic development. Studies of the African clawed frog, *Xenopus laevis*, have shown that members of the transforming growth factor β and fibroblast growth factor (FGF) families are essential for mesodermal tissue differentiation and for coordinating cell movements associated with gastrulation (22, 49, 51). Both of these processes can be studied ex vivo in *Xenopus* animal caps (ectodermal explants). Stimulation of animal caps with activin (a transforming growth factor β family member) induces a wide range of tissues, including (depending on the dose) dorsal and ventral mesoderm, neural tissue, and endoderm. The induced dorsal mesoderm undergoes convergence and extension movements (reviewed in reference 51), which drive dramatic elongation of the animal caps. In embryos, these movements provide the primary motive force for gastrulation. FGF family members induce a more restricted range of tissues in animal caps, including ventrolateral mesodermal derivatives such as muscle, mesenchyme, and mesothelium, but do not induce neural tissue, endoderm, or dorsal mesodermal structures, such as notochord (24). FGF stimulation also causes shape changes in animal caps, but FGF-induced elongation is distinct from that evoked by activin. It has been assumed that one or more of the tissues induced by FGF drive FGF-stimulated elongation. However, it has not been shown explicitly that FGF-stimulated elongation depends on FGF-induced differentiation. Additionally, the cellular behaviors that lead to FGF-induced animal cap elongation, as well as the signaling pathways downstream of the *Xenopus* FGF receptor (XFGFR) that control it, are not well understood (51). The precise role of FGF-induced movements in embryogenesis also is unclear.

Some downstream signals required for FGF-stimulated mesoderm induction have been identified. For example, inhibition of members of the signaling cassette that includes Ras, Raf, MEK, and mitogen-activated protein kinase (MAPK) prevents mesoderm induction by FGF. Moreover, expression of activated forms of these molecules (in the absence of additional stimuli) induces mesodermal genes and the formation of muscle, mesenchyme, and mesothelium (13, 32, 35, 59, 63). The protein-tyrosine phosphatase (PTP) SHP-2 also is required for FGF signaling in *Xenopus*. Embryos expressing a dominant inhibitory form of SHP-2 (ΔP) develop normal heads, but trunk and tail development is defective due to incomplete gastrulation (55). Animal caps expressing ΔP fail to elongate when stimulated with FGF (or activin), and induction of the mesodermal markers Xbra and muscle actin is blocked (55). Thus, like MAPK cascade components, SHP-2 is required for FGF-stimulated mesodermal gene induction and for elongation movements in animal caps.

Multiple studies indicate that SHP-2 function is required for MAPK activation in response to a variety of growth factors. However, its precise position in the pathway leading to MAPK activation remains controversial (38, 61); some studies suggest that SHP-2 also acts in parallel to the MAPK pathway (1, 15, 36, 65). Although SHP-2 is required for FGF-induced MAPK activation in *Xenopus* (41, 55), it remains unclear whether SHP-2 activation is sufficient to stimulate the MAPK pathway and/or to evoke elongation movements and mesoderm induction.

To resolve these issues, we took advantage of recent insights into the structure and mechanism of activation of SHP-2 to generate novel, activated mutants. SHP-2 contains two SH2 domains, a catalytic (PTP) domain and a C-terminal tail of unknown function (38, 61) (Fig. 1). In the absence of an appropriate phosphotyrosyl peptide ligand for its N-terminal SH2

* Corresponding author. Mailing address: HIM 1047, Beth Israel-Deaconess Medical Center, 330 Brookline Ave., Boston, MA 02215. Phone: (617) 667-2823. Fax: (617) 667-0610. E-mail: bneel@caregroup.harvard.edu.

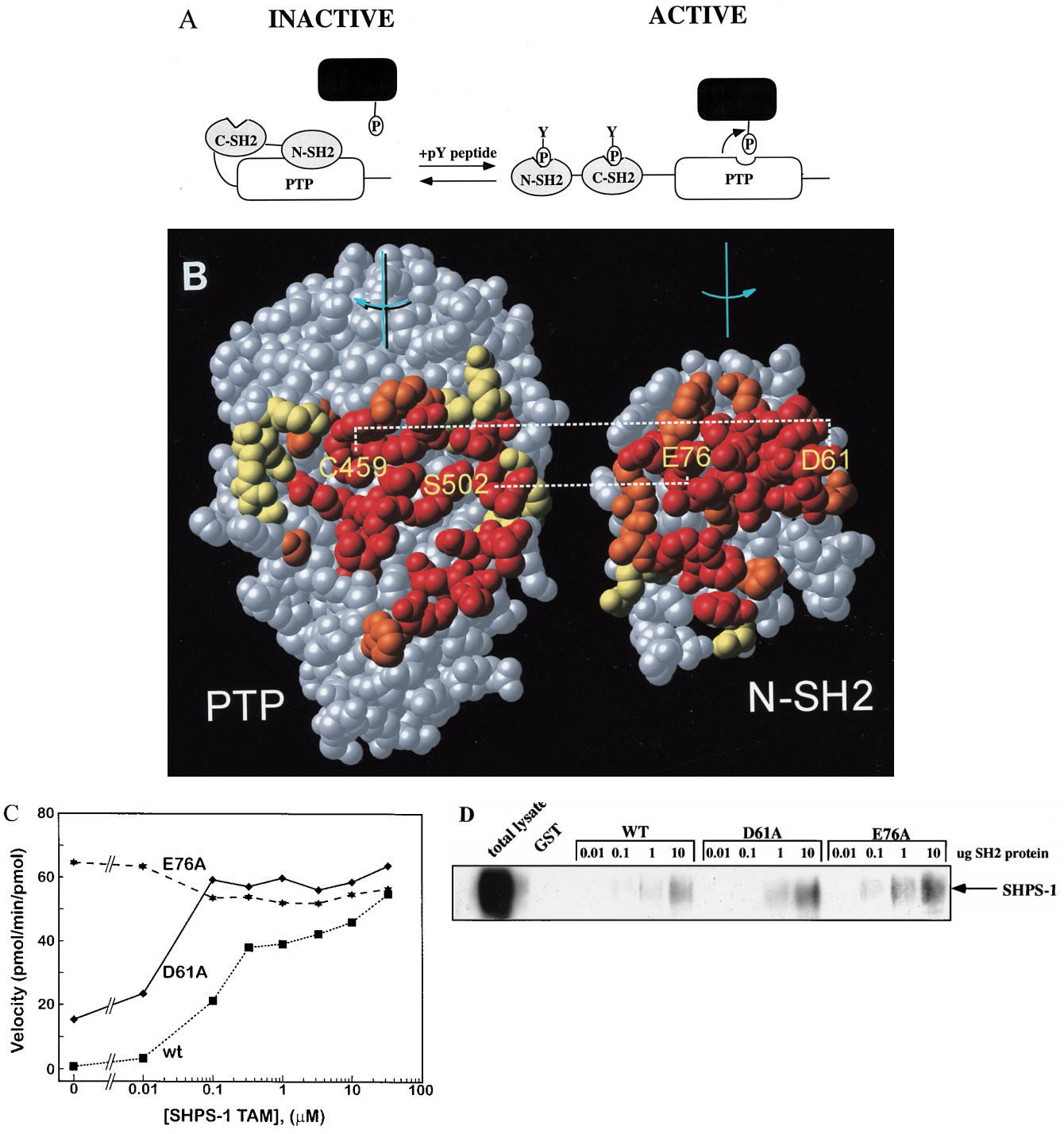

FIG. 1. Generation of activated mutants of SHP-2. (A) Schematic diagram of regulation of SHP-2 activity as proposed by Hof et al. (19). (B) "Open-book" view of binding surfaces. The PTP domain (left) and N-SH2 (right) are both rotated 90° but in opposite directions to expose the buried surface between them. Contact residues are color coded to reflect the percentage of surface buried (red, 50 to 100%; orange, 25 to 50%; yellow, 0 to 25%). Hydrogen bonding interactions between D61 and C459 and between E76 and S502 are indicated by dashed lines. (C) Catalytic activity of activated mutants. Specific activities (picomoles of ^{32}P released per minute per picomole) of wild-type (wt) D61A, and E76A proteins are plotted versus SHPS-1 ligand concentration. (D) Pull-down experiments using increasing amounts of wild-type (WT) or mutant (D61A or E76A) GST–N-SH2 domain fusion proteins to bind endogenous tyrosyl-phosphorylated SHPS-1 from J77 macrophage cell lysates. Immunoblots of precipitated material were probed with anti-SHPS-1 antibodies.

(N-SH2) domain, SHP-2 has virtually no enzymatic activity; addition of an appropriate ligand results in dramatic activation (3). The crystal structure of SHP-2 provides a molecular explanation for these phenomena. In the basal state, the N-SH2 domain binds to the active site of the PTP domain, physically and chemically inactivating the enzyme (19). Ligand binding to the N-SH2 domain prevents its binding to the PTP domain, thereby activating the enzyme (Fig. 1A). The N-SH2 residues

that bind to the PTP domain reside on the surface opposite from the phosphotyrosyl peptide binding pocket. These structural features raised the possibility of generating variant forms of SHP-2 that lose basal inhibition yet retain phosphotyrosyl peptide binding.

In this study, we generated and characterized the biological properties of two such mutants. Expression of these mutants in animal caps induces elongation to an extent equivalent to that evoked by addition of exogenous FGF. Interestingly, however, unlike FGF and activated versions of MAPK pathway components, activated mutants of SHP-2 induce weak or undetectable activation of MAPK, mesodermal markers, and mesodermal cytodifferentiation. These results suggest that the pathways downstream of the XFGFR that direct elongation movements and mesodermal differentiation may be separable and that SHP-2 preferentially activates the former pathway(s). We also identify potential downstream elements of the pathway directing elongation in response to SHP-2 activation.

MATERIALS AND METHODS

Mutant construction. D61A, E76A, and KKDA were constructed by overlap extension PCR using human SHP-2 cDNA as the template. For D61A, oligonucleotides 5′-GGT CAT AGT AAG CAC TGT TC-3′ (D61Aa) and 5′-CG GAA TTC AAC ATG ACA TCG CGG AG-3′ (Ek1s) were used to generate a 200-bp fragment containing the 5′ end, and oligonucleotides 5′-G AAC ACT GGT GCT TAC TAT GAC C-3′ (D61As) and the standard T3 primer were used to generate the 1.8-kb 3′ end of the construct. The above products were used in a second PCR with Ek1s and T3 to generate the full-length 2.0-kb product, which was blunt-end cloned into pBluescript KS (Stratagene) and subcloned into *Eco*RI-digested pSp64R1 (55) or pGEX 4T (Pharmacia). E76A was cloned via an analogous strategy, using the oligonucleotide sets 5′-CTG GAC CAA CGC AGC CAA AGT G-3′ (E76Aa) plus Ek1s and 5′-C ACT TTG GCT GCG TTG GTC CAG-3′ (E76As) plus T3, respectively, for first-round reactions. KKDA was cloned by using the same primers and PCR conditions as used for cloning D61A, but the template was R32,138K (41). N-SH2 domain constructs were generated by PCR. Wild-type SHP-2, D61A, or E76A served as the template for reactions primed at the N terminus of SHP-2 and the C-terminal end of the N-SH2 domain (primers available upon request from S. Pluskey). PCR products were subcloned into *Eco*RI-digested pGEX 4T.

Production and purification of SHP-2. *Escherichia coli* BL21/DE3 transformed with pGEX 4T-2 constructs encoding wild-type or mutant SHP-2, either full length or N-SH2 domains, were grown to an optical density of 0.6 to 0.8 and induced with 0.1 μM isopropyl-β-D-thiogalactopyranoside. Following harvesting and cell lysis, recombinant proteins were collected on glutathione-Sepharose, eluted with 20 mM glutathione, and dialyzed in 25 mM Tris (pH 8.0)–150 mM NaCl–10 mM dithiothreitol. For purification of full-length SHP-2, fusion proteins were cleaved by thrombin and Ca^{2+} (2.5 mM), and cleavage products were purified by fast protein liquid chromatography (Mono Q) to greater than 97% homogeneity as shown by sodium dodecyl sulfate-polyacrylamide gel electrophoresis.

PTP assays. SHPS-1 peptide DIT(pY)ADLNLPKGKKPAPQAAEPNNH TE(pY)ASIQTS-NH2 (pY indicates phosphotyrosine) was synthesized by using previously described methods (42). Reduced carboxyamidomethylated and maleylated lysozyme (RCML) was phosphorylated to a specific activity of approximately 2,000 cpm/pmol by recombinant Src (gift from W. Xu, Harvard Medical School) essentially as described elsewhere (42). PTP assays were carried out in the presence of the indicated SHP-2 protein (1 to 5 nM) and SHPS-1 peptide (0 to 33 mM) as described elsewhere (42).

Analysis of SH2 domain binding. Cell pellets from J77 macrophages (gift from John F. Timms, Beth Israel Deaconess Medical Center) were lysed in NP-40 lysis buffer (1% NP-40, 50 mM Tris [pH 7.4], 150 mM NaCl), containing protease inhibitors (10 μg of leupeptin per ml, 1 μg of aprotinin per ml, 1 μg of pepstatin A per ml, 1 μg of antipain per ml, and 20 μg of phenylmethylsulfonyl fluoride per ml) and 2 mM sodium vanadate and incubated on ice for 10 min. Lysates were clarified for 15 min at 45,000 rpm at 4°C. Protein concentrations were determined by the bicinchoninic acid assay (Pierce). Increasing glutathione *S*-transferase (GST)–N-SH2 domain fusion proteins (see above and figure legends) were incubated with 500 μg of J77 lysate for 1.5 h at 4°C; 25 μl of a 50% slurry of glutathione-agarose was then added, and mixtures were incubated for 30 min at 4°C. Samples were briefly precipitated by centrifugation and washed four times in lysis buffer. Beads were resuspended in 1× sample buffer, electophoresed, and transferred onto Immobilon-P membranes. Immunoblots were probed with rabbit polyclonal anti-SHPS-1 antibodies (57).

Plasmid constructs and in vitro transcription. SHP-2 constructs, activated MEK (MEK*) (32), dominant negative Ras (63) (MEK* and DNRas; gifts from M. Whitman, Harvard Medical School), dominant negative C-cadherin (C-trunc [33]) (gift from B. Gumbiner, Memorial Sloan-Kettering Cancer Center and Cornell Medical School), embryonic FGF (23) (gift from H. Isaacs, University of Bath), and Xbra-EnR (7) (gift from J. Smith, National Institute for Medical Research) were linearized and subjected to in vitro transcription using SP6 polymerase and a MEGAscript kit (Ambion). Dominant negative Rho (Rho19N; subcloned from pZIP-rhoA-19N [27]) (gift from C. Der, University of North Carolina, Chapel Hill) was excised from pZIP by digestion with *Eco*RI and subcloned into *Eco*RI-linearized pXT7SRI (54). pXT7SRI-Rho19N was linearized and subjected to in vitro transcription using T7 polymerase and a MEGAscript kit (Ambion).

Embryo manipulations. Fertilization and embryo culture were performed as described previously (55). RNA (10 nl) was injected into both cells of two-cell embryos at the animal pole. Animal caps were excised at stage 7.5–8.5 and analyzed as described previously (55).

Histology. Stage 39 animal caps were fixed, sectioned, and stained with hematoxylin and eosin (55) or with Feulgan/light green/orange G (Sigma) as described elsewhere (14).

RNA analysis. RNA extraction and Northern analysis of muscle actin were performed as described elsewhere (55). For analysis of early markers, RNA was isolated from stage 10-11 animal caps (see figure legends). RNA isolated from stage 21 animal caps was used for analysis of the late marker NCAM. Reverse transcription (RT)-PCR was performed essentially as described previously (21) except that oligo(dT) (Gibco-BRL) was used to prime the RT reactions. Primer sequences for ODC, Xbra, Xwnt-8, goosecoid (Gsc), and NCAM are available online (http://vize222.zo.utexas.edu). Primers for mixer (17), sox17α (21), and sox17β (21) were as described elsewhere. Primers for pintallavis (U-AGGTCT CTCTAATGACGG and D-TGTCTGCATGTCTAGTCC) were based on unique sequences within its cDNA. The annealing temperature was 55°C for all reactions. Cycle numbers were as follows: ODC, 18; Xbra, pintallavis, sox17α, sox17β, mixer, and Xwnt-8, 23; Gsc and NCAM, 27.

Protein analysis. MAPK assays were performed as described previously (41) except that animal caps were lysed in 1× sample buffer instead of 1% NP-40 lysis buffer. Dissociated cells were stimulated either by addition of 100 ng of exogenous FGF (human basic FGF [bFGF, Upstate Biotechnology, Inc.] or XbFGF [gift from K. Itoh and S. Sokol, Beth Israel Deaconess Medical Center) per ml or by raising the temperature of animal caps expressing activated SHP-2 mutants to 24°C for 5 min. Immunoblots were probed with anti-ERK2 antibodies (Santa Cruz Biotechnology). SHP-2 expression was analyzed by using anti-SHP-2 monoclonal antibodies (Transduction Laboratories).

RESULTS

We generated two activated forms of SHP-2 by mutating N-SH2 domain residues (aspartate 61 [D61] or glutamate 76 [E76]) that form key contacts with the PTP domain (19) (Fig. 1B). Our goal was to generate mutants that would target correctly within cells yet be activated by subthreshold levels of stimulation. We produced the two mutant proteins in *E. coli*, purified them, and assayed their enzymological properties. Both were basally activated in vitro (Fig. 1C), although to different extents. Relative to wild-type SHP-2, D61A exhibited approximately 20-fold higher basal activity against the artificial substrate tyrosyl-phosphorylated RCML. Addition of a phosphotyrosyl peptide ligand for the N-SH2 domain led to further activation of D61A in a ligand concentration-dependent manner (Fig. 1C). In contrast, E76A was fully activated (~100-fold) in the absence of any added ligand. The increased activation of D61A upon ligand binding strongly suggested that this mutant retains a functional N-SH2 phosphotyrosyl binding pocket. However, to confirm that both of the mutant N-SH2 domains retain wild-type phosphotyrosyl protein-binding ability, we generated GST–N-SH2 fusion proteins for wild-type SHP-2, D61A, and E76A and compared their abilities to bind a known ligand for the N-SH2 of SHP-2, SHPS-1 (12, 26, 44, 64). All three N-SH2 domains bound to SHPS-1 with approximately equal affinities (Fig. 1D), indicating that neither the D61A nor the E76A mutation disrupts the N-SH2 phosphotyrosyl binding pocket. This conclusion is further supported by in vitro binding studies with phosphotyrosyl peptides (data not shown). Therefore, we conclude that mutation of D61 or E76 weakens the basal interaction between the N-SH2 and PTP domains, leading to enzymatic activation without affecting ligand binding.

We next assessed the biological activity of the activated

SHP-2 mutants in animal cap assays. Untreated animal caps remain spherical. Treatment with an appropriate peptide growth factor results in elongation, characterized by distortion of the spherical shape of the animal cap (49). As expected, animal caps stimulated with FGF elongated at stage 11-11.5 in a dose-dependent manner (49) (Fig. 2A). Overexpression of wild-type SHP-2 in the absence of FGF does not evoke animal cap elongation (55) (see Fig. 4A). In contrast, expression of either D61A or E76A induced substantial elongation in the absence of exogenous growth factors (Fig. 2A). The extent of elongation depended on SHP-2 protein levels: low levels of D61A induced detectable but slight elongation, whereas higher levels evoked elongation indistinguishable from that produced by FGF stimulation (Fig. 2A, lower panel). In contrast, E76A-expressing animal caps elongated at most doses tested (Fig. 2A), consistent with the higher catalytic activity of this mutant (Fig. 1C). Importantly, expression of a form of D61A in which the essential FLVRES arginines in both SH2 domains are mutated to lysines (KKDA) failed to evoke elongation (Fig. 2B). This result implies that phosphotyrosyl protein binding and, presumably, appropriate subcellular targeting of SHP-2 are required for activated mutant function.

The requirement for a functional phosphotyrosyl binding pocket also implies that at least one ligand for the SH2 domains of SHP-2 must be phosphorylated in unstimulated animal caps. Previous studies have demonstrated that FGF is present and that low-level constitutive stimulation of the XFGFR pathway occurs in unstimulated animal caps (24). In addition, our previous work established that SHP-2 function is required for XFGFR signaling (41, 55). Thus, it seemed possible, if not likely, that the activated mutants function to enhance low-level signaling through the XFGFR pathway. Such a model implies that XFGFR function should be required for activated mutant-induced elongation. To test this possibility, we inhibited endogenous XFGFR activity by expressing a dominant negative form of the XFGFR (XFD) that lacks the cytoplasmic domain (2). The dose of XFD used in these experiments blocked FGF-induced animal cap elongation (data not shown), indicating that we had inhibited XFGFR activity. Moreover, elongation induced by either D61A or E76A also was inhibited by XFD coexpression (Fig. 3), demonstrating that basal FGF signaling is required for the action of the activated SHP-2 mutants. These results further support the conclusion that D61A and E76A mimic the endogenous SHP-2 signaling pathway in animal caps.

In addition to evoking elongation, FGF stimulation promotes expression of mesodermal markers and differentiation of animal cap ectoderm to ventrolateral mesoderm (see the introduction). We therefore expected that like FGF treatment (51), expression of the activated SHP-2 mutants would evoke tissue differentiation concomitant with animal cap elongation and, indeed, that the induced mesodermal derivatives might drive elongation movements. We looked for evidence of such tissues in animal caps expressing the activated mutants. E76A expression induced low levels of mesodermal tissue, including a mesothelial layer and mesenchyme (Fig. 4A and B). Thus, high levels of SHP-2 (e.g., as generated by E76A) can evoke some (low) level of mesodermal tissue differentiation, consistent with weak activation of the full range of FGF signaling events by E76A. Surprisingly, however, no mesodermally derived tissues were detected in D61A-expressing animal caps (Fig. 4A and B). D61A-expressing animal caps displayed numerous vacuoles, but these structures were clearly distinct from those associated with notochord (Fig. 3B); their origin remains unknown. As expected, FGF-stimulated caps contained muscle and other ventrolateral mesodermal derivatives, including mesothelium and mesenchyme (Fig. 4A and B), whereas activin-stimulated animal caps developed dorsal structures, including notochord and neural tissue (Fig. 4B). Thus, D61A-expressing animal caps elongate fully (i.e., comparably

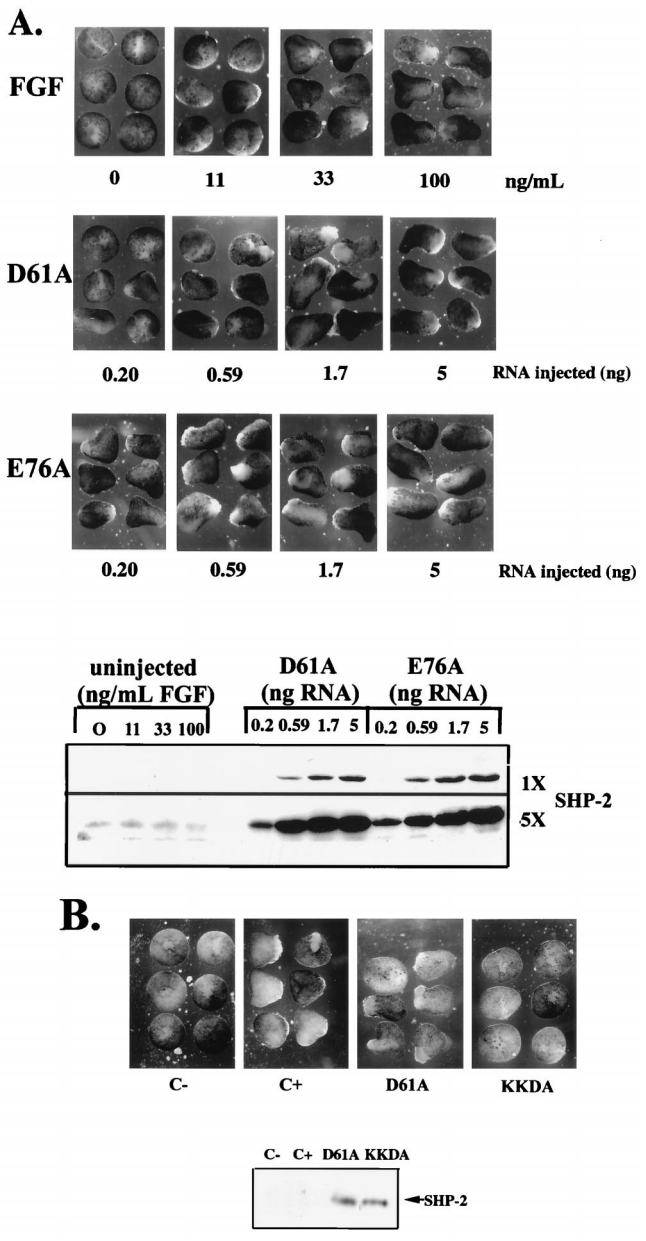

FIG. 2. Expression of activated mutants induces elongation of *Xenopus* animal caps. (A) (Top panel) Stage 8 animal caps were stimulated with increasing concentrations of FGF, as indicated. Photographs were taken at stage 11.5 to assess elongation. (Second panel) Animal caps were isolated from embryos injected with threefold serial dilutions of D61A mRNA. No exogenous stimulus was applied, and elongation was assessed as above. (Third panel) Animal caps were isolated from embryos injected with the indicated dilutions of E76A in the absence of additional stimuli and analyzed as above. (Bottom panel) Levels of expression of the D61A and E76A proteins in this experiment. Two exposures of the SHP-2 immunoblot, representing fivefold differences in exposure time, are shown to indicate the relative level of expression of the activated mutants compared with endogenous SHP-2. (B) Animal caps were isolated from either uninjected embryos or embryos injected with D61A or KKDA RNA (1.7 ng). Uninjected animal caps were either left unstimulated (C−) or stimulated with FGF (100 ng/ml; Upstate Biotechnology, Inc.) (C+). No exogenous stimulus was applied to animal caps injected with D61A or KKDA RNA. Elongation was assessed as above.

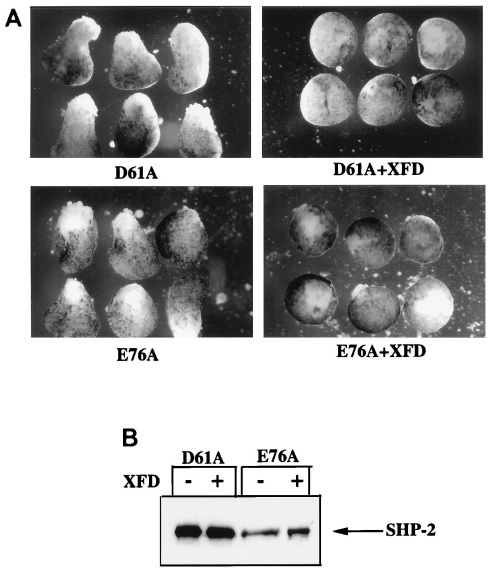

FIG. 3. A functional XFGFR is required for the effects of the activated SHP-2 mutants. (A) Animal caps were injected with 5 ng of either D61A or E76A RNA (left) or coinjected with the indicated activated SHP-2 mutant and XFD (2.5 ng) (right). (B) Protein levels for D61A and E76A. Control experiments indicated that the dose of XFD used was sufficient to inhibit all FGF signaling in animal caps (data not shown).

to FGF-stimulated animal caps) yet fail to exhibit significant (or even detectable) evidence of mesodermal cytodifferentiation.

In addition to mesodermal derivatives, such as notochord and muscle, neural tissue and endoderm also can contribute to elongation movements in animal caps (17, 25). D61A-expressing animal caps exhibited a yolky appearance, characteristic of either endoderm or lack of tissue differentiation. However, molecular marker analysis (see below and Fig. 4F) strongly suggests that no endodermal differentiation occurs in D61A (or E76A)-injected animal caps. Furthermore, in contrast to activin-stimulated animal caps, there was no histological evidence of neural differentiation in response to activated mutant expression (Fig. 4B).

We further analyzed differentiation in animal caps expressing the activated mutants by surveying the expression of molecular markers. The late mesodermal marker muscle actin was detected on Northern blots following FGF stimulation and, to a markedly lower degree, upon E76A expression. However, in agreement with the histological sections (Fig. 4A and B), no muscle actin mRNA was detected in D61A-expressing animal caps (Fig. 4C). We also analyzed early marker expression by RT-PCR. As expected, FGF stimulated Xbra expression in a dose-dependent manner. Notably, doses of FGF (11 ng/ml) that did not induce elongation stimulated significant Xbra expression (Fig. 4D). Also as expected, expression of an activated form of MEK (MEK*) (32), a downstream effector in the FGF pathway, induced Xbra expression (Fig. 4D). In contrast, at low doses of E76A, no Xbra mRNA was detected (Fig. 4D), although such doses were capable of inducing elongation comparably to FGF (Fig. 2A). At higher levels of expression, E76A did evoke significant Xbra expression. However, Xbra was induced barely, if at all, by even the highest levels of D61A expression (Fig. 4D). Again, it should be emphasized that these animal caps elongated dramatically (Fig. 2A and data not shown). Interestingly, one FGF-regulated gene, Xwnt-8, was induced significantly by both activated mutants (Fig. 4D), raising the possibility that Xwnt-8 participates in a pathway selectively induced by SHP-2 action. Thus, expression of activated forms of SHP-2 in animal caps leads to induction of some but not all FGF-mediated downstream events.

Consistent with the lack of histological evidence of neural differentiation, there was no detectable expression of NCAM in activated mutant-expressing animal caps (Fig. 4E). Furthermore, there was no expression of the endodermal marker mixer, sox-17α, or sox17β (Fig. 4F), arguing that the activated mutants do not induce endoderm. Elongation induced by the activated mutants probably is not due to gratuitous activation of the activin signaling pathway, since we did not detect expression of several activin-induced genes, including Gsc, pintallavis (Fig. 4E), and the early endodermal markers discussed above (Fig. 4F).

We next looked at earlier signaling events. FGF stimulation results in the rapid activation of MAPK. To assess the effects of the activated mutants on the MAPK pathway, we took advantage of the fact that D61A- and E76A-expressing animal caps exhibited cold sensitivity: mutant-expressing animal caps failed to elongate at 13°C, whereas incubation at higher temperatures resulted in elongation (Fig. 5A and data not shown). Injected embryos were incubated at 13°C until stage 8. Cells from dissociated animal caps were then stimulated by acutely raising the temperature to 24°C in the presence or absence of FGF. Under these conditions, E76A activated MAPK (as indicated by reduction in electrophoretic mobility) in a dose-dependent manner, whereas activation of D61A resulted in minimal, often undetectable MAPK activation (Fig. 5B). When animal caps expressing either activated mutant were maintained at 13°C, no MAPK activation was observed, and expression of wild-type SHP-2 failed to activate MAPK at any temperature tested (data not shown).

These data indicate that elongation can occur with minimal activation of MAPK. Moreover, activation of MAPK by FGF was not sufficient to induce maximal elongation. Stimulation of uninjected animal caps with either 11 or 100 ng of FGF per ml significantly activated MAPK (Fig. 5B), yet only animal caps stimulated with the higher dose elongated fully (Fig. 2). In contrast, animal caps expressing D61A elongated dramatically, but MAPK activation was minimal (Fig. 2 and 5B). These results suggest that FGF-stimulated animal cap elongation may require activation of a parallel pathway that is regulated preferentially by SHP-2.

Overexpression of Xbra in animal caps induces mesoderm (9). However, the minimal activation of MAPK and Xbra transcription by activated SHP-2 mutants, which evoke strong elongation, raised the possibility that Xbra expression per se might be dispensable for FGF-induced elongation movements. Xbra function can be inhibited effectively by expression of a fusion of the DNA binding domain of Xbra with the repressor domain from *Drosophila engrailed* (Xbra-EnR) (7). Coexpression of Xbra-EnR and E76A led to complete inhibition of Xbra transcription (data not shown) and prevented E76A-induced elongation (Fig. 6).

At first glance, this result appears to imply that at least some Xbra function is required for both mesoderm induction and elongation. However, in animal caps, the relationship between XFGFR signaling and Xbra is complex. XFGFR activation leads to Xbra transcription (24, 50). Xbra in turn induces transcription of the gene for the XFGFR ligand eFGF (47). This results in a positive feedback loop that maintains FGF signaling throughout early mesoderm induction and gastrulation (24, 47) (see Discussion). XFD blocks mesoderm induction evoked by overexpression of Xbra, demonstrating the importance of this feedback loop (47). Because the activated

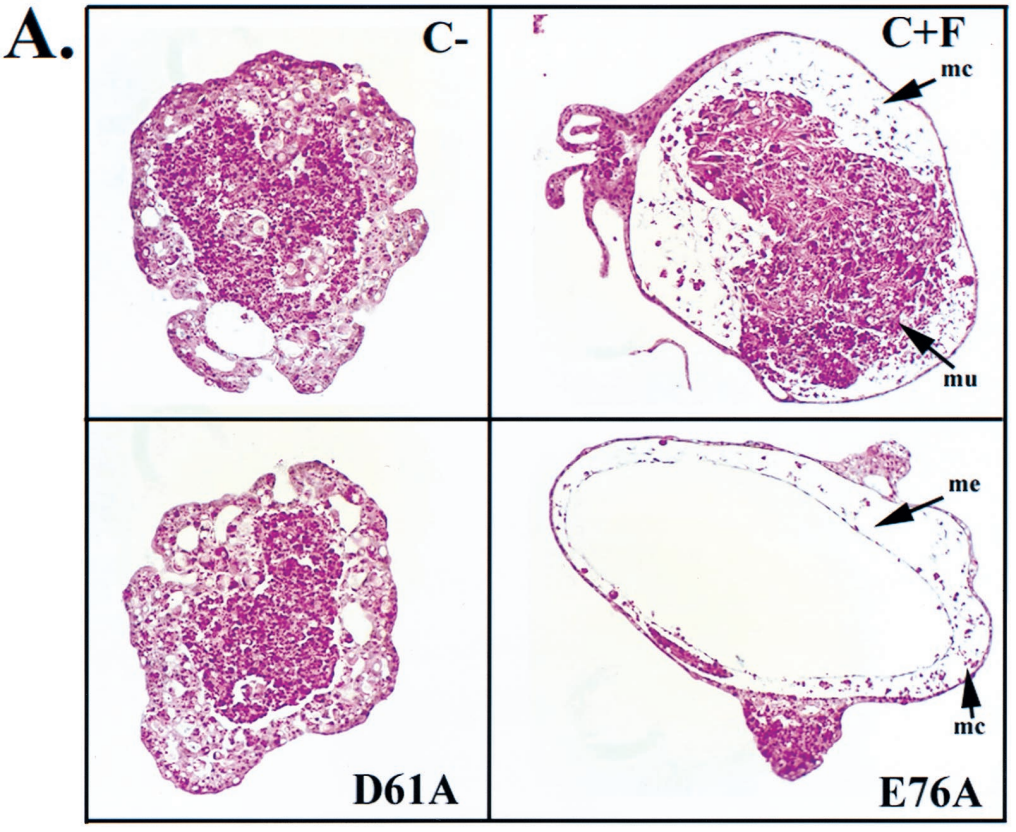
A.
C-
C+F
mc
mu
me
mc
D61A
E76A

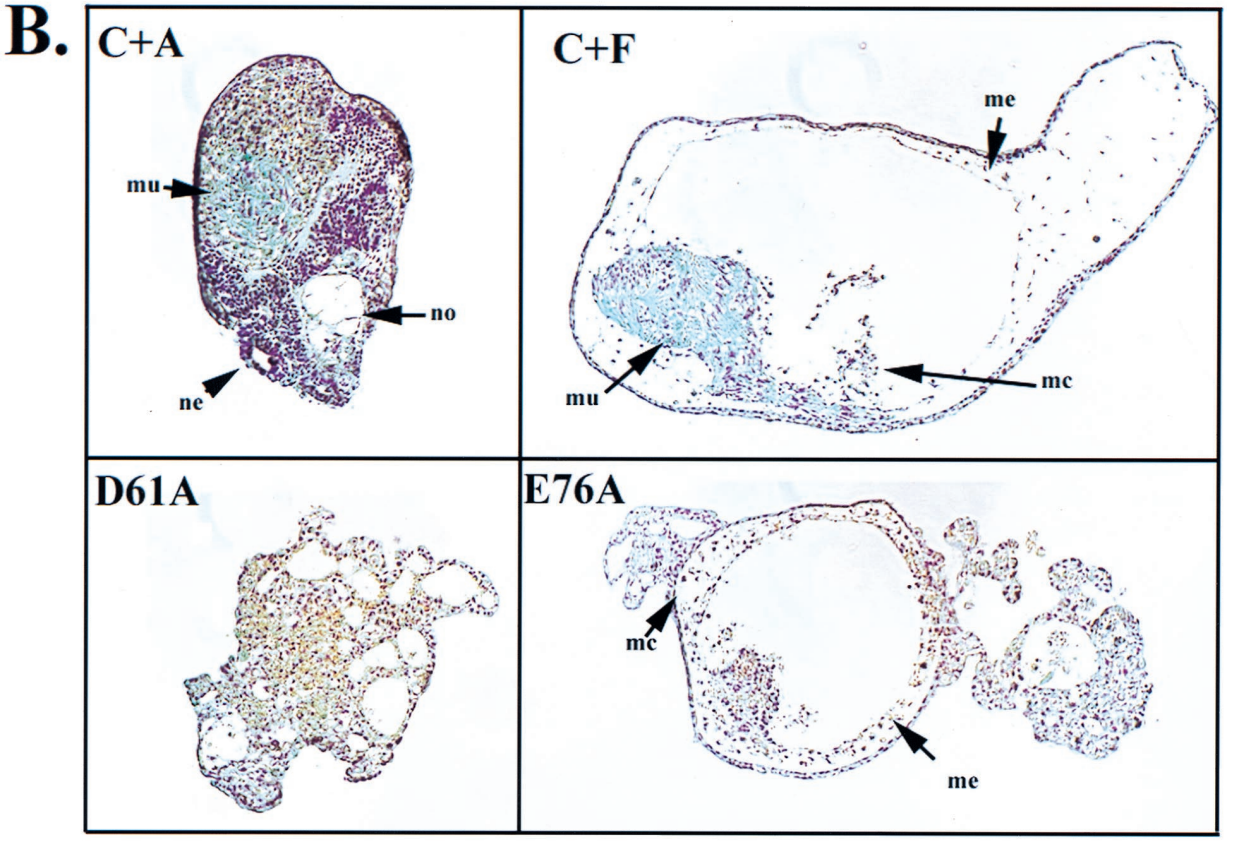
B.
C+A
mu
no
ne
C+F
me
mu
mc
D61A
E76A
mc
me

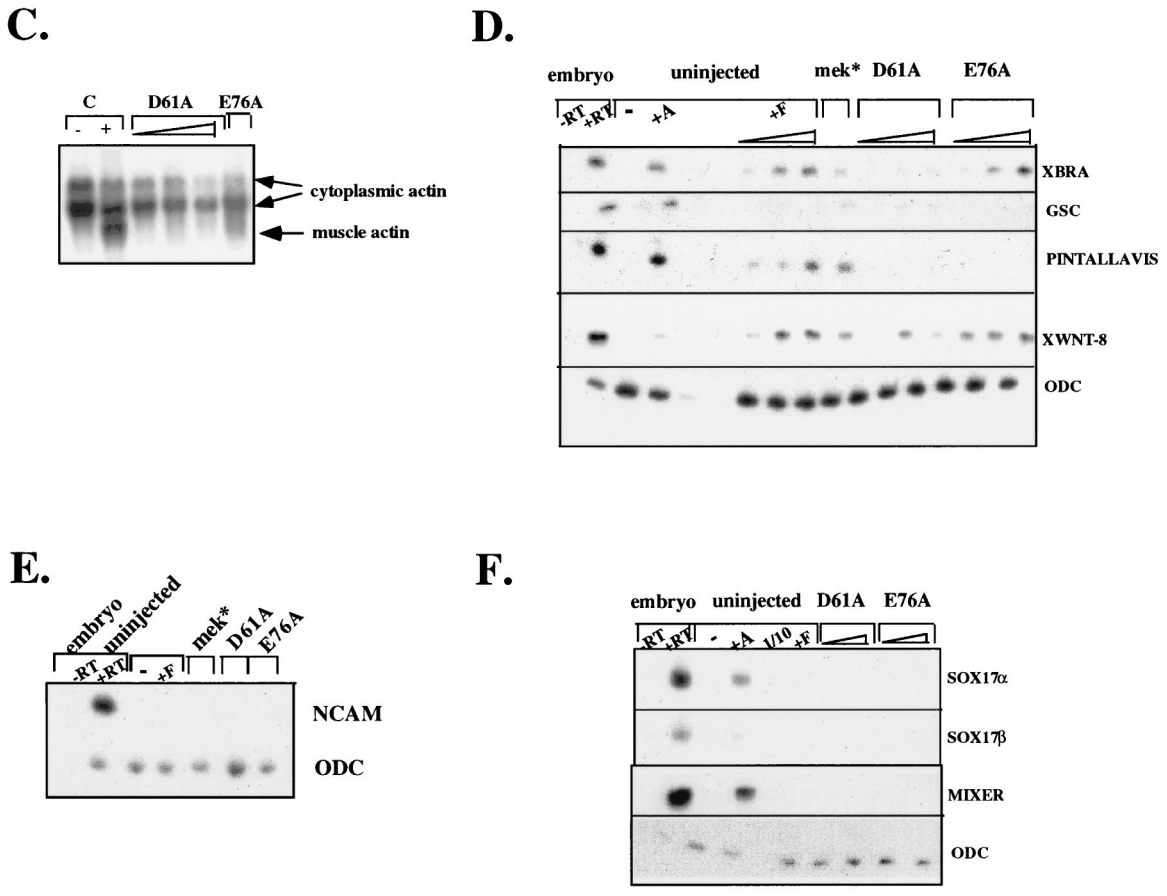

FIG. 4. Analysis of differentiation in animal caps expressing activated mutants of SHP-2. (A and B) Histological sections from stage 39 animal caps that were unstimulated (C−) or stimulated with activin (5 ng/ml) (C+A) or FGF (100 ng/ml) (C+F) or expressing D61A or E76A. The levels of D61A and E76A protein in these animal caps were equivalent (data not shown). Sections were stained with hematoxylin and eosin (A) or Feulgan/light green/orange G (B). Notochord (no), neural tissue (ne), muscle (mu), mesothelium (me), and mesenchyme (mc) are indicated. (C) Northern analysis of the late mesodermal marker muscle actin. Animal caps collected at stage 21 were analyzed for muscle actin mRNA (lowest band). The two upper bands represent cytoplasmic actin, which cross-reacts with the probe and serves as a loading control. The mRNA injected is indicated above each lane. The triangle under D61A represents successive threefold dilutions of D61A RNA, with the maximal dose being 5 ng. (D) RT-PCR analysis of stage 11 animal caps. Animal caps were stimulated with activin (+A, 5 ng/ml) or threefold dilutions of FGF (+F), with the highest concentration being 100 ng/ml. Alternatively, animal caps were injected with fivefold dilutions of D61A or E76A mRNA, with the maximum injection being 5 ng, or with 50 ng of activated MEK (mek*) RNA, in the absence of any additional stimulation. RNA was isolated from animal caps or normal embryos at stage 11 and subjected to RT-PCR analysis with the indicated primers as described in Materials and Methods. All of the markers in this panel were isolated from a single experiment; ODC expression served as a loading control for all markers. Similar results were obtained in a minimum of three independent experiments. −RT indicates negative control RT-PCR reactions carried out in the absence of reverse transcriptase. Note that similar results were observed when RNA was isolated at stage 10. (E) RT-PCR analysis of NCAM expression in stage 21 animal caps expressing the indicated proteins or left uninjected. ODC serves as a control for equal loading. (F) RT-PCR analysis of endodermal marker expression in stage 11 animal caps isolated as for panel D.

mutants require an N-SH2 ligand for activity, and generation of this ligand requires XFGFR function (see above), the inhibitory effect of Xbra-EnR could be due to failure to generate eFGF. To test this possibility, we coexpressed E76A and Xbra-EnR and provided exogenous FGF to the media in order to bypass the FGF feedback loop. Addition of FGF to the media did not rescue induction of elongation by E76A (data not shown), suggesting either that Xbra is directly required for elongation to occur or that exogenous FGF is not stable enough to provide a continuous signal throughout the assay. To allow continuous production of ligand, we next coinjected RNAs encoding E76A, Xbra-EnR, and the XFGFR ligand, eFGF (23). Although the dose of eFGF used was sufficient to induce MAPK activation (Fig. 6B) and Xbra expression (data not shown), eFGF did not rescue E76A-induced animal cap elongation (Fig. 6A). These results clearly demonstrate that Xbra function is required for elongation in response to activated mutants of SHP-2. However, since D61A and low doses of E76A do not induce Xbra to a significant extent, these results indicate that the amount of Xbra required for elongation is much lower than that required for mesodermal tissue differentiation (see Discussion).

We previously showed that SHP-2 activity is required for FGF-induced MAPK activation, Xbra induction, and elongation (55). However, activated mutants of SHP-2 are, at best, weak inducers of MAPK activation and Xbra expression. These results imply that XFGFR activation sends additional signals to yield full MAPK activation. To determine if such signals combine with SHP-2 to enhance MAPK activation, we asked whether subthreshold levels of FGF and D61A or E76A would synergize. To test this prediction, we established doses of FGF and D61A or E76A RNA that lead to minimal induction of elongation, MAPK activation, and Xbra induction (Fig. 7). When animal caps expressing low-dose D61A or E76A were stimulated with low-dose FGF, markedly enhanced elon-

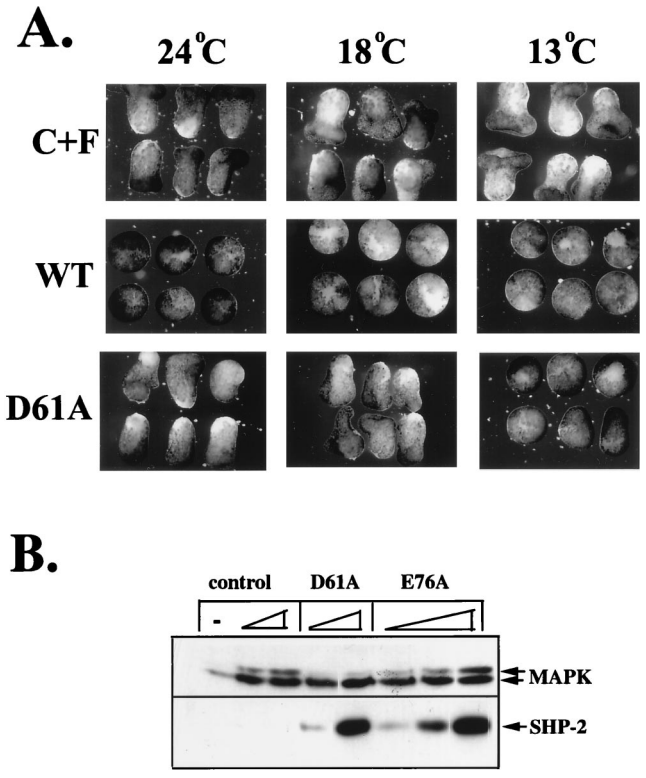

FIG. 5. Activated mutants induce minimal MAPK activation. (A) Cold sensitivity of D61A mutant. Embryos were injected with wild-type (WT) or D61A RNA (5 ng) at the two-cell stage and cultured at 13°C until stage 8. Animal caps were excised and then incubated at the indicated temperatures. C+F, uninjected plus FGF (100 ng/ml). (B) Immunoblot analysis of injected animal caps at stage 8. Total lysates from animal caps injected with activated mutant RNA, as indicated, in the absence of any additional stimulation, or from uninjected caps stimulated with the indicated concentrations of FGF were probed with anti-ERK2 or anti-SHP-2 antibodies. MAPK activation is indicated by a decrease in electrophoretic mobility.

gation (Fig. 7A), MAPK activation (Fig. 7B), and Xbra induction (Fig. 7C and data not shown) were observed.

Finally, we sought to identify downstream components of FGF- or activated SHP-2-mediated signaling leading to elongation. Previous reports have demonstrated a requirement for Ras downstream of the XFGFR. Consistent with these data, expression of dominant negative Ras (63) (DNRas) blocked FGF-dependent elongation (Fig. 8A), as well as MAPK activation (Fig. 8B) and Xbra induction (Fig. 8C). Similarly, DNRas completely abolished elongation movements induced by E76A (Fig. 8A). This result is consistent with the notion that Xbra induction by signaling through the Ras/Raf/MAPK cascade is required for E76A-dependent elongation. The weak E76A-dependent induction of MAPK (data not shown) and Xbra (Fig. 8C) also was completely inhibited by coexpression with DNRas.

Activin-stimulated morphogenetic movements are dependent on regulation of C-cadherin-mediated cell-cell adhesion (5, 33). We examined whether C-cadherin also plays a role in FGF- and E76A-induced elongation. Interestingly, expression of a dominant negative form of C-cadherin that lacks its cytoplasmic domain (C-trunc) (33) did not prevent either FGF- or E76A-induced elongation (Fig. 8A). The same dose of C-trunc dramatically reduced activin-stimulated morphogenetic movements (data not shown), as reported previously (33).

Recently, SHP-2 has been implicated in regulation of the actin cytoskeleton in tissue culture cells (40, 65). The small G protein Rho regulates actin cytoskeleton reorganization (56) and is required for completion of gastrulation in *Drosophila* (4, 16). Expression of dominant negative Rho (Rho19N) (27) completely abolished FGF- and E76A-induced elongation (Fig. 8A). In contrast to the results seen upon expression of DNRas, Rho19N expression had no effect on MAPK activation or induction of Xbra by either FGF or E76A (Fig. 8B and C). These findings indicate that Rho acts downstream of SHP-2 in the pathway leading to elongation.

DISCUSSION

FGF treatment of *Xenopus* animal caps has two main biological effects, mesoderm induction and elongation movements (24). XFGFR stimulation results in the activation of multiple downstream signaling molecules. Which of these signal relay molecules is important for the biological actions of FGF in animal caps is unclear. Previous studies have shown that multiple components of the MAPK cascade are necessary and sufficient for mesoderm induction and elongation (24). SHP-2 also is known to be required for both processes, as well as for activation of MAPK (41, 55). However, it had not been clear whether SHP-2 is sufficient for either mesoderm induction or elongation.

To answer this question, we generated two novel, activated forms of SHP-2 by mutating critical N-SH2 residues that me-

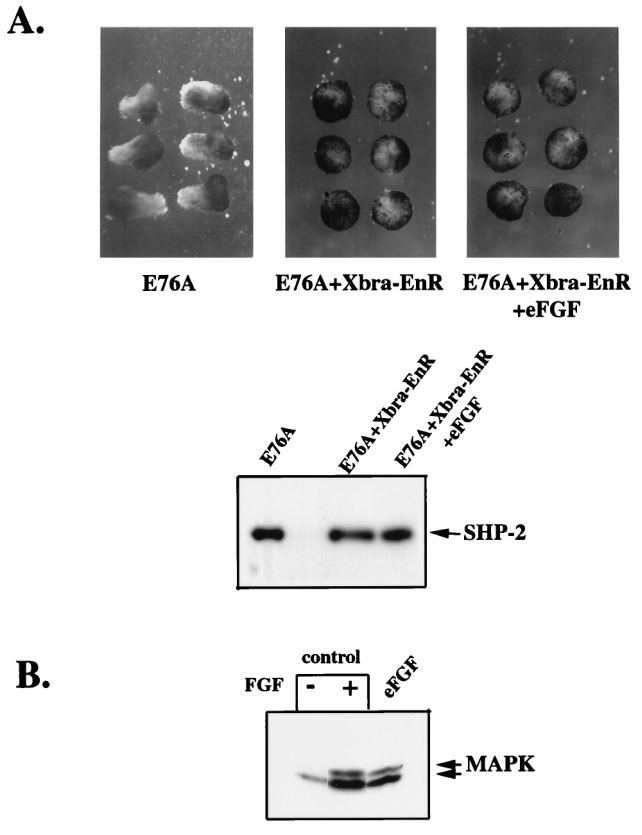

FIG. 6. Inhibition of Xbra activity prevents activated mutant-induced elongation. (A) Animal caps injected with E76A (5 ng), E76A (5 ng) and Xbra-EnR (200 pg), or E76A (5 ng), Xbra-EnR (200 pg), and eFGF (5 pg) were left unstimulated and allowed to develop until stage 11.5, when elongation was scored. (B) MAPK activation was assessed as in Fig. 5 in animal caps left unstimulated, stimulated with 100 ng of FGF per ml, or injected with 5 pg of eFGF.

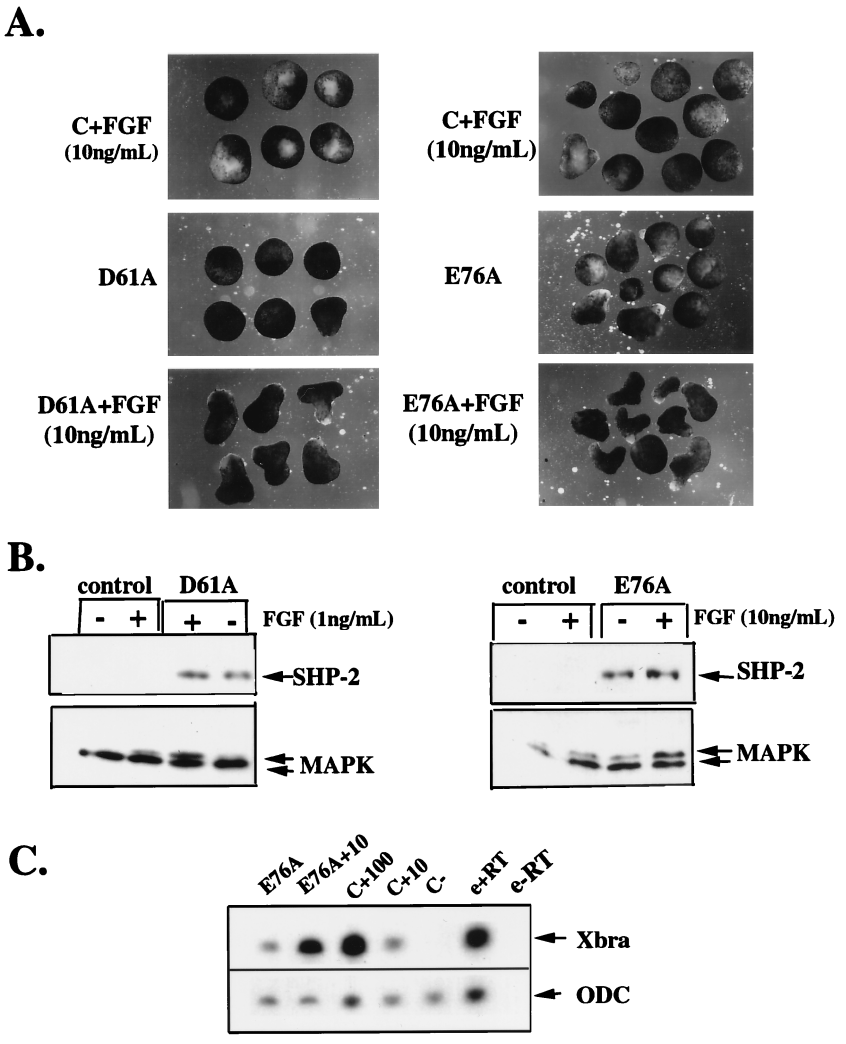

FIG. 7. Activated SHP-2 mutants synergize with FGF. (A) Animal caps were either uninjected (top panel) or injected with 0.2 ng of D61A (left side, middle panel) or 0.2 ng E76A (right side, middle panel). Uninjected animal caps (top panel) or activated mutant-injected animal caps (bottom panel) were stimulated with exogenously added FGF (11 ng/ml) and analyzed for elongation as in Fig. 2. (B) Total lysates from animal caps injected with D61A (left panel) or E76A (right panel) or from uninjected or activated mutant-injected animal caps stimulated with the indicated concentrations of FGF were probed with anti-ERK2 or anti-SHP-2 antibodies. (C) RNA was isolated from stage 10 animal caps (treated as indicated) and subjected to RT-PCR analysis using a primer for Xbra or ODC (see Materials and Methods). E76A+10, injected with E76A and stimulated with FGF (10 ng/ml); C+100, uninjected plus FGF (100 ng/ml); C+10, uninjected plus FGF (10 ng/ml); C−, uninjected controls; e+RT, stage 10 embryos plus reverse transcriptase; e−RT, stage 10 embryos with no reverse transcriptase.

diate basal inhibition. Strikingly, both activated mutants induce elongation to a degree indistinguishable from that induced by saturating doses of FGF, but in the absence of exogenously added growth factor. In contrast, activation of MAPK (for D61A in particular), induction of early and late mesodermal markers, and mesodermal cytodifferentiation are minimal or absent. Thus, our data indicate that the pathways controlling mesoderm induction and elongation in response to FGF are at least partially separable and that activated forms of SHP-2 preferentially activate a pathway(s) downstream of the XFGFR that leads to elongation. In further support of this idea, Rho is essential for FGF- and E76A-induced elongation but not for activation of MAPK or Xbra induction.

The crystal structure of SHP-2 (19) strongly suggests that basal inhibition of catalytic activity is mediated by interaction between the N-SH2 and PTP domains. Although multiple contacts exist between these domains (19), mutation of either D61 or E76 in the N-SH2 domain is sufficient to generate activated mutants. This suggests either that these two residues participate in particularly important interactions with the PTP domain or that nearly all of the contacts are needed to maintain basal inhibition. In wild-type SHP-2, E76 forms a hydrogen bond with S502 in the PTP domain, whereas D61 participates in a hydrogen bonding network to the catalytic cysteine (19). The relative strengths of these interactions probably account for the different basal activities of these mutants (Fig. 1B). Importantly, however, both mutants retain the ability to bind appropriate SH2 domain ligands (Fig. 1C). Our data thus provide strong support for the physiological relevance of the model for SHP-2 regulation based on its crystal structure (19). In addition, although C-terminal truncations of PTP-1B (11) and T-cell PTP (8, 34) result in enhanced catalytic activity, these mutations remove the targeting sequence within these PTPs. Our activated mutants represent the first examples of PTP gain-of-function mutations that retain appropriate intracellular targeting capability.

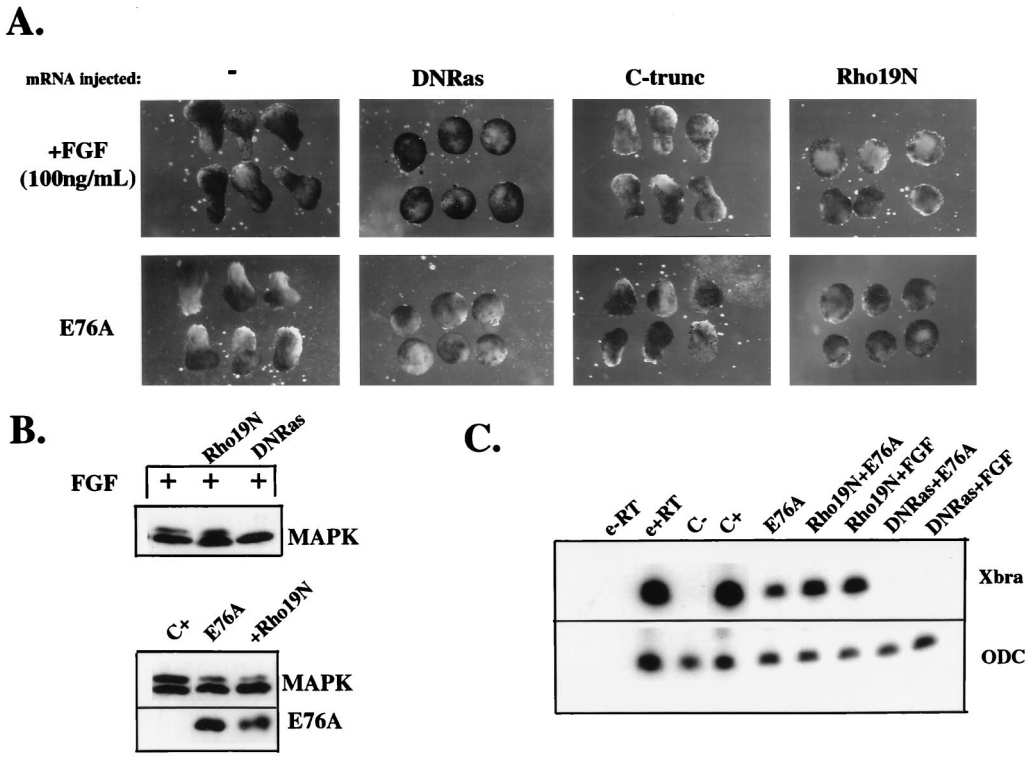

FIG. 8. Pathways required for signaling by activated SHP-2 mutants. (A) Animal caps injected with RNA encoding DNRas (64) (5 ng), C-trunc (33) (20 pg), or Rho19N (100 pg), as indicated, were analyzed for elongation after either stimulation with FGF (100 ng/ml) or coinjection with E76A (5 ng). (B) Analysis of the effects of DNRas and Rho19N on MAPK activation induced either by FGF (above) or expression of E76A (below). Total lysates were probed with anti-ERK2 or anti SHP-2 antibodies as in Fig. 5. (C) RNA was isolated from stage 10 animal caps injected with the indicated RNAs (see legend to panel A for amounts) and subjected to RT-PCR analysis using primers for Xbra or ODC, as indicated. Lanes are labeled as in Fig. 7C.

Several lines of evidence indicate that the biological effects of our activated mutants mimic those of physiologically activated SHP-2. First, the activated mutants are biologically active only if they retain SH2 domain function (Fig. 2B), suggesting that the mutants and endogenous SHP-2 act at similar sites. Second, D61A- and E76A-induced elongation requires signaling through the XFGFR (Fig. 3), the same signaling pathway in which endogenous SHP-2 participates (41, 55). Third, the activated mutants synergize with subthreshold levels of exogenous FGF, enhancing the full panel of FGF-induced events in animal caps (Fig. 7).

The most striking effect of both activated SHP-2 mutants is their ability to induce animal cap elongation to an extent comparable to that of FGF. The mechanism by which FGF controls cell movements in animal caps (and in embryos) is not well understood, although cell movements induced by activin have been studied extensively. Activin stimulates convergence and extension of the cells in animal caps, mimicking the movements of mesodermal cells undergoing gastrulation (54). These morphogenetic movements require C-cadherin-mediated cell-cell adhesion (reference 5 and 31 and data not shown). In contrast, we find that inhibition of C-cadherin activity has no effect on elongation evoked either by FGF or E76A (Fig. 8A). Thus, our results imply that FGF- and activin-induced cell movement pathways are, at least partially, distinct.

The mechanistic details of the FGF-induced movement pathways remain to be elucidated. Conceivably, other cadherins implicated in activin-induced cell movements, such as U-cadherin (30) or paraxial protocadherin (28), are required for FGF- or E76A-induced elongation. Notably, the *Drosophila* homolog of SHP-2, Csw, binds to a scaffolding molecule, Dos (18), which localizes to adherens junctions (43); recent evidence indicates that a mammalian relative of Dos, Gab-1, which binds to SHP-2 (20), also is located at cell-cell junctions (62). Association with these scaffolding molecules may help target SHP-2 to key substrates within points of cell-cell contact, allowing SHP-2 to regulate adhesive events. Alternatively, or in addition, SHP-2 may regulate shape changes and/or cell movement by associating with adhesion molecules such as SHPS-1/SIRPα (12, 26). Recent work indicates that SHP-2, most likely acting via SHPS-1–SHP-2 complexes, regulates integrin-dependent signaling events in mammalian fibroblasts (40, 45, 58, 65). Our activated mutants of SHP-2 may provide useful reagents for identifying downstream components of FGF-induced cell movement pathways. Such pathways may be of general importance in development, since SHP-2 plays an important role in control of growth factor- and integrin-induced cell movements in mammalian cells and embryos (36, 40, 45, 46, 65; and T. Saxton, B. Ciruna, D. Holmyard, S. Kulkarni, K. Harpal, J. Rossant, and T. Pawson, submitted for publication).

Surprisingly, activated mutants induce full elongation (i.e., compared with FGF) in the absence of significant induction of mesodermal markers and/or mesodermal cytodifferentiation. Importantly, we have shown that our mutants do not gratuitously induce other types of tissue (e.g., endoderm or neural tissue) that might drive elongation movements (Fig. 4). Therefore, we conclude that neither expression of the full panel of FGF-induced mesodermal markers nor histological evidence of mesodermal differentiation is requisite for inducing cell

movements leading to elongation of animal caps. However, our results also show that the pathways to mesodermal gene induction/cytodifferentiation and elongation are not completely separable. Because Xbra-EnR blocks activated mutant-induced elongation, even in the presence of exogenously or endogenously supplied FGF (Fig. 6), at least some level of Xbra function is required for elongation. Notably, elongation movements induced by most doses of D61A or low doses of E76A occur in the absence of detectable Xbra mRNA, even when this is monitored by the highly sensitive RT-PCR assay. This finding suggests that either maternal Xbra protein (52) or the level of Xbra generated by endogenous FGF signaling (and below the level of detection of our RT-PCR assay) is sufficient to subserve this function. Regardless, however, the level of Xbra required for D61A- or E76A-dependent elongation is far lower than that required for mesodermal differentiation.

One marker, Xwnt-8, was induced comparably in response to activated mutant expression or FGF stimulation. Thus, Xwnt-8 may lie on a signaling pathway downstream from SHP-2. Activated mutant expression appears to generate a premesodermal (or partial mesodermal) state in which animal cap ectodermal cells take on some mesodermal characteristics (e.g., cell movement capability and Xwnt 8 expression) but not others (e.g., Xbra, muscle actin expression, and tissue differentiation). Intriguingly, previous studies have shown that overexpression of Xwnt-8 induces animal cap elongation and ventral mesoderm (53). However, Xwnt-8 induces elongation of only animal caps cut at later stages than those used for FGF- or activated mutant-induced elongation (10, 53). A tantalizing possibility is that one FGF-induced signaling event, perhaps acting through the MAPK pathway, cooperates with Xwnt-8, which is activated via an FGF/SHP-2 signaling pathway.

Our results also yield insights into the position of SHP-2 in XFGFR signaling. Previously, we showed that dominant negative mutants of SHP-2 block FGF-induced MAPK activation (41, 55). Subsequent studies using primary fibroblasts or fibroblastic cell lines from SHP-2 exon 3 mutant mice confirmed these observations (46, 48). Moreover, a wide variety of studies using both dominant negative mutants and SHP-2 mutant fibroblasts have shown that SHP-2 function is required for full activation of MAPK in response to growth factors, cytokines, antigen receptors, and integrin engagement. However, whether SHP-2 lies upstream or downstream of Ras has remained controversial (37, 38, 61). Our activated mutants allowed us to perform epistasis experiments, in which we demonstrated that DNRas prevents all effects of the activated mutants (Fig. 8 and data not shown). The simplest interpretation of these results is that SHP-2 acts directly upstream of the Ras/Raf/MEK/MAPK cascade. This notion also is consistent with direct assessments of the effect of dominant negative SHP-2 mutants on Ras loading in response to insulin (39) and other growth factors (H. Liu and B. G. Neel, unpublished observations), analyses of the effects of growth factor receptors unable to bind SHP-2 or its homologs (6, 29), and the general agreement that SHP-2 acts upstream of MAPK (see above).

However, D61A and low doses of E76A only weakly activate MAPK (compared to the level of activation evoked by FGF treatment), whereas they fully evoke elongation. Conceivably, the amount of Ras activation needed to evoke elongation is less than that needed to activate MAPK. In that case, activated SHP-2 mutants would be capable of inducing a (low) level of Ras loading, but further activation of SHP-2 through generation of additional phosphorylated targets for its SH2 domains upon FGF stimulation would be needed to generate levels of Ras sufficient to fully activate the MAPK pathway. A second possibility is that SHP-2 cooperates with a major FGF-stimulated pathway to further enhance the level of Ras activation. For example, SHP-2 may regulate targeting or activation of RasGAP, thereby abrogating Ras inactivation, consistent with studies in other systems (6, 29). Alternatively, SHP-2 might regulate a Ras exchange protein. A third possibility is that in the XFGFR pathway, SHP-2 acts upstream of MAPK but completely in parallel to Ras activation. Although formally possible, such a model would imply that SHP-2 helps activate MAPK via distinct mechanisms downstream of different growth factor receptors. Notably, all of these models are consistent with our finding that stimulation of D61A- or E76A-expressing animal caps with FGF leads to dramatic synergy for MAPK activation.

One interpretation of our results, and the model we favor, is that the level of MAPK activation required for induction of elongation movements (which can be fully evoked by activated mutants of SHP-2) is substantially less than that stimulated by maximal FGF treatment of animal caps or that required to fully induce mesodermal markers and cytodifferentiation. However, we measured MAPK activation at stage 8, which is considerably earlier than the time at which elongation movements occur (stage 10.5-11). Conceivably, the activated mutants lead to stronger MAPK activation at some later time point; future studies will address this issue. Nevertheless, previous studies established that after stage 9 (32), animal caps lose their ability to induce MAPK upon FGF stimulation, thus defining a window within which activated SHP-2 mutants probably act. Activated SHP2 mutants also induce Xbra poorly under most conditions. Xbra is induced by MAPK activation and induction occurs significantly after FGF treatment (at stage 10). If activated SHP2 mutants fully induce MAPK, but at a later time point, one might expect Xbra to be induced to comparable levels by activated mutants and FGF.

Finally, additional epistasis experiments strongly suggest that the small G protein Rho is an essential downstream component of FGF- and activated SHP-2 mutant-induced elongation. Consistent with its role in cell movements in animal caps, Rho regulates rearrangements of the actin cytoskeleton that permit cell movement in multiple tissue culture systems (56) and is required for cell movements in gastrulating *Drosophila* embryos (4, 16). Notably, and in contrast to the actions of dominant negative Ras or SHP-2, Rho19N prevents FGF- and activated mutant-induced animal cap elongation without affecting MAPK activation or Xbra induction (Fig. 8). Thus, Rho acts downstream of XFGFR and SHP-2 in a pathway leading to elongation, and this pathway is distinct from the XFGFR/SHP-2-mediated pathway to MAPK activation and Xbra induction. Interestingly, p190RhoGAP is a tyrosyl phosphoprotein (60) and thus represents a potential SHP-2 target. However, our data also are consistent with models in which Rho is activated far downstream of SHP-2 and participates in elongation as a late event. Further work will be required to elucidate the mechanism by which SHP-2 regulates Rho, as well as to delineate other components of the FGF-induced elongation pathway. The activated mutants described herein should prove useful for such experiments, as well as for studies aimed at delineating the direct roles of SHP-2 in other signaling systems and cell types.

ACKNOWLEDGMENTS

We thank W. Xu (Harvard Medical School), M. Whitman (Harvard Medical School), G. L. Henry (Harvard University) B. Gumbiner (Memorial Sloan-Kettering Cancer Center), C. Der (University of North Carolina, Chapel Hill), H. Isaacs (University of Bath), J. Smith (National Institute for Medical Research), and J. Timms (Beth Israel Deaconess Medical Center) for generous gifts of reagents, K. Itoh and

S. Sokol (Beth Israel Deaconess Medical Center and Harvard Medical School) for FGF and frogs, D. Goodenough (Harvard Medical School), J. Green (Dana-Farber Cancer Institute), and K. Symes (Boston University School of Medicine) for help with histological analyses, M. Mercola and M. Kirschner (Harvard Medical School), S. Sokol (Beth Israel Deaconess Medical Center), C. Carpenter (Beth Israel Deaconess Medical Center), J. Green (Dana-Farber Cancer Institute), K. Symes (Boston University School of Medicine), and S. Thomas (Beth Israel Deaconess Medical Center) for helpful discussions and critical reading of the manuscript, and S. Cohen for help with manuscript preparation.

This work was supported by grants from the NIH (RO1 CA49152 to B.G.N. and RO1 DK45943, RO1 DK51729 to S.E.S.) and the Burroughs Wellcome Fund Scholar Award in Experimental Therapeutics (to S.E.S.).

REFERENCES

1. **Allard, J. D., H. C. Chang, R. Herbst, H. McNeill, and M. A. Simon.** 1996. The SH2-containing tyrosine phosphatase corkscrew is required during signaling by sevenless, Ras1 and Raf. Development **122:**1137–1146.
2. **Amaya, E., T. J. Musci, and M. W. Kirschner.** 1991. Expression of a dominant negative mutant of the FGF receptor disrupts mesoderm formation in *Xenopus* embryos. Cell **66:**257–260.
3. **Barford, D., and B. G. Neel.** 1998. Revealing mechanisms for SH2 domain-mediated regulation of the protein tyrosine phosphatase SHP-2. Structure **6:**249–254.
4. **Barrett, K., M. Leptin, and J. Settleman.** 1997. The Rho GTPase and a putative RhoGEF mediate a signaling pathway for the cell shape changes in *Drosophila* gastrulation. Cell **91:**905–915.
5. **Brieher, W., and B. Gumbiner.** 1994. Regulation of C-Cadherin function during activin induced morphogenesis of *Xenopus* animal caps. J. Cell Biol. **126:**519–527.
6. **Cleghon, V., U. Gayko, T. D. Copeland, L. A. Perkins, N. Perrimon, and D. K. Morrison.** 1996. Drosophila terminal structure development is regulated by the compensatory activities of positive and negative phosphotyrosine signaling sites on the Torso RTK. Genes Dev. **10:**566–577.
7. **Conlon, F., S. Sedgwick, K. Weston, and J. Smith.** 1996. Inhibition of Xbra transcription activation causes defects in mesodermal patterning and reveals autoregulation of Xbra in dorsal mesoderm. Development **122:**2427–2435.
8. **Cool, D. E., P. R. Andreassen, N. K. Tonks, E. G. Krebs, E. H. Fischer, and R. L. Margolis.** 1992. Cytokinetic failure and asynchronous nuclear division in BHK cells overexpressing a truncated protein-tyrosine-phosphatase. Proc. Natl. Acad. Sci. USA **89:**5422–5426.
9. **Cunliffe, V., and J. Smith.** 1992. Ectopic mesoderm formation in *Xenopus* embryos caused by widespread expression of a Brachyury homolgue. Nature **358:**427–430.
10. **Cunliffe, V., and J. Smith.** 1994. Specification of mesodermal pattern in *Xenopus laevis* by interactions between *Brachyury*, *noggin*, and *Xwnt-8*. EMBO J. **13:**349–359.
11. **Frangioni, J. V., P. H. Beahm, V. Shifrin, C. A. Jost, and B. G. Neel.** 1992. The nontransmembrane tyrosine phosphatase PTP-1B localizes to the Endoplasmic reticulum via its 35 amino acid C-terminal sequence. Cell **68:**545–560.
12. **Fujioka, Y., T. Matozaki, T. Noguchi, A. Iwamatsu, T. Yamao, N. Takahashi, M. Tsuda, T. Takada, and M. Kasuga.** 1996. A novel membrane glycoprotein, SHPS-1, that binds the SH2-domain-containing protein tyrosine phosphatase SHP-2 in response to mitogens and cell adhesion. Mol. Cell. Biol. **16:**6887–6899.
13. **Gotoh, Y., N. Masuyama, A. Suzuki, N. Ueno, and E. Nishida.** 1995. Involvement of the MAP kinase cascade in Xenopus mesoderm induction. EMBO J. **14:**2491–2498.
14. **Green, J., G. Howes, K. Symes, J. Cooke, and J. Smith.** 1990. The biological effects of XTC-MIF: quantitative comparison with *Xenopus* bFGF. Development **108:**173–183.
15. **Gu, H., J. C. Pratt, S. J. Burakoff, and B. G. Neel.** 1998. Cloning and characterization of the major SHP-2 binding protein in hematopoietic cells (p97) reveals a novel pathway for cytokine-induced gene activation. Mol. Cell **2:**729–740.
16. **Hacker, U., and N. Perrimon.** 1998. *DRhoGEF2* encodes a member of the Dbl family of oncogenes and controls cell shape changes during gastrulation in *Drosophila*. Genes Dev. **12:**274–284.
17. **Henry, G., and D. Melton.** 1998. Mixer, a homeobox gene required for endoderm development. Science **281:**91–96.
18. **Herbst, R., P. M. Carroll, J. D. Allard, J. Schilling, T. Raabe, and M. A. Simon.** 1996. Daughter of Sevenless is a substrate of the phosphotyrosine phosphatase corkscrew and functions during Sevenless signaling. Cell **85:**899–909.
19. **Hof, P., S. Pluskey, S. Dhe-Paganon, M. J. Eck, and S. E. Shoelson.** 1998. Crystal structure of the SH2 domain phosphatase SHP-2. Cell **98:**441–450.
20. **Holgado-Madruga, M., D. R. Emlet, D. K. Moscatello, A. K. Godwin, and A. J. Wong.** 1996. A Grb2-associated docking protein in EGF- and insulin-receptor signalling. Nature **379:**560–564.
21. **Hudson, C., D. Clements, R. Friday, D. Stott, and H. Woodland.** 1997. Xsox17α and -β mediate endoderm formation in *Xenopus*. Cell **91:**397–405.
22. **Isaacs, H., M. Pownall, and J. Slack.** 1994. eFGF regulates *Xbra* expression during *Xenopus* gastrulation. EMBO J. **13:**4469–4481.
23. **Isaacs, H., D. Tannahill, and J. Slack.** 1992. Expression of a novel FGF in the *Xenopus* embryo. A new candidate inducing factor for mesoderm formation and anteroposterior specification. Development **114:**711–720.
24. **Isaacs, H. V.** 1997. New perspectives on the role of the fibroblast growth factor family in amphibian development. Cell. Mol. Life Sci. **53:**350–361.
25. **Keller, R., and R. Winklbauer.** 1992. Cellular basis of amphibian gastrulation. Curr. Top. Dev. Biol. **27:**39–89.
26. **Kharitonenkov, A., Z. Chen, I. Sures, H. Wang, J. Schilling, and A. Ullrich.** 1997. A family of proteins that inhibit signaling though tyrosine kinase receptors. Nature **386:**181–186.
27. **Khosravi-Far, R., P. Solski, G. Clark, M. Kinch, and C. Der.** 1995. Activation of Rac1, RhoA, and mitogen-activated protein kinases is required for Ras transformation. Mol. Cell. Biol. **15:**6443–6453.
28. **Kim, S.-H., A. Yamamoto, T. Bouwmeester, E. Agius, and E. De Robertis.** 1998. The role of Paraxial Protocadherin in selective adhesion and cell movements of the mesoderm during *Xenopus* gastrulation. Development **125:**4681–4691.
29. **Klinghoffer, R. A., and A. Kazlauskas.** 1995. Identification of a putative Syp substrate, the PDGFβ receptor. J. Biol. Chem. **270:**22208–22217.
30. **Kuhl, M., S. Finnemann, O. Binder, and D. Wedlich.** 1996. Dominant negative expression of a cytoplasmically deleted mutant of XB/U-cadherin disturbs mesoderm migration during gastrulation in *Xenopus laevis*. Mech. Dev. **54:**71–82.
31. **Kuhl, M., and D. Wedlich.** 1996. Xenopus cadherins: sorting out types and functions in embryogenesis. Dev. Dyn. **207:**121–134.
32. **LaBonne, C., B. Burke, and M. Whitman.** 1995. Role of MAP kinase in mesoderm induction and axial patterning during *Xenopus* development. Development **121:**1475–1486.
33. **Lee, C.-H., and B. M. Gumbiner.** 1995. Disruption of gastrulation movements in Xenopus by a dominant-negative mutant for C-cadherin. Dev. Biol. **171:**363–373.
34. **Lorenzen, J. A., C. Y. Dadabay, and E. H. Fischer.** 1995. COOH-terminal sequence motifs target the T cell protein tyrosine phosphatase to the ER and nucleus. J. Cell Biol. **131:**631–643.
35. **MacNicol, A. M., A. J. Muslin, and L. T. Williams.** 1993. Raf-1 kinase is essential for early *Xenopus* development and mediates the induction of mesoderm by FGF. Cell **73:**571–583.
36. **Manes, S., E. Mira, C. Gomes-Mouton, Z. Zhao, R. Lacalle, and C. Martines-A.** 1999. Concerted activity of tyrosine phosphatase SHP-2 and focal adhesion kinase in regulation of cell motility. Mol. Cell. Biol. **19:**3125–3135.
37. **Neel, B. G.** 1997. Role of phosphatases in lymphocyte activation. Curr. Opin. Immunol. **9:**405–420.
38. **Neel, B. G., and N. K. Tonks.** 1997. Protein tyrosine phosphatases in signal transduction. Curr. Opin. Cell Biol. **9:**193–204.
39. **Noguchi, T., T. Matozaki, K. Horita, Y. Fujioka, and M. Kasuga.** 1994. Role of SH-PTP2, a protein-tyrosine phosphatase with Src homology 2 domains, in insulin-stimulated *ras* activation. Mol. Cell. Biol. **14:**6674–6682.
40. **Oh, E.-S., H. Gu, T. Saxton, J. Timms, S. Hausdorff, E. Frevert, B. Kahn, T. Pawson, B. Neel, and S. Thomas.** 1999. Regulation of early events in integrin signaling by the protein-tyrosine phosphatase SHP-2. Mol. Cell. Biol. **19:**3205–3215.
41. **O'Reilly, A. M., and B. G. Neel.** 1998. Structural determinants of SHP-2 function and specificity in *Xenopus* mesoderm induction. Mol. Cell. Biol. **18:**161–177.
42. **Pluskey, S., T. J. Wandless, C. T. Walsh, and S. E. Shoelson.** 1995. Potent stimulation of SH-PTP2 phosphatase activity by simultaneous occupancy of both SH2 domains. J. Biol. Chem. **270:**2987–2900.
43. **Raabe, T., J. Riesgo-Escovar, X. Liu, B. S. Bausenwein, P. Deak, P. Maroy, and E. Hafen.** 1996. DOS, a novel pleckstrin homology domain-containing protein required for signal transduction between sevenless and Ras1 in Drosophila. Cell **85:**911–920.
44. **Sano, S., H. Ohnishi, A. Omori, J. Hasegawa, and M. Kubota.** 1997. BIT, an immune antigen receptor-like molecule in the brain. FEBS Lett. **411:**327–334.
45. **Saxton, T., and T. Pawson.** 1999. Morphogenetic movements at gastrulation require the SH2 tyrosine phosphatase Shp2. Proc. Natl. Acad. Sci. USA **96:**3790–3795.
46. **Saxton, T. M., M. Henkemeyer, S. Gasca, R. Shen, D. J. Rossi, F. Shalaby, G.-S. Feng, and T. Pawson.** 1997. Abnormal mesoderm patterning in mouse embryos mutant for the SH2 tyrosine phosphatase SHP-2. EMBO J. **16:**2352–2364.
47. **Schulte-Merker, S., and J. Smith.** 1995. Mesoderm formation in response to *Brachyury* requires FGF signalling. Curr. Biol. **5:**62–67.
48. **Shi, Z.-Q., W. Lu, and G.-S. Feng.** 1998. The Shp-2 tyrosine phosphatase has opposite effects in mediating the activation of extracellular signal-regulated

and c-Jun NH_2-terminal mitogen-activated protein kinases. J. Biol. Chem. **273:**4904–4908.
49. **Smith, J. C.** 1995. Mesoderm-inducing factors and mesodermal patterning. Curr. Opin. Cell Biol. **7:**856–861.
50. **Smith, J. C.** 1993. Mesoderm-inducing factors in early vertebrate development. EMBO J. **12:**4463–4470.
51. **Smith, J. C., and J. E. Howard.** 1992. Mesoderm-inducing factors and the control of gastrulation. Dev. Suppl. **1992:**127–136.
52. **Smith, J. C., B. M. J. Price, J. B. A. Green, D. Weigel, and B. G. Herrmann.** 1991. Expression of a Xenopus homolog of *Brachyury (T)* is an immediate-early response to mesoderm induction. Cell **67:**79–87.
53. **Sokol, S. Y.** 1993. Mesoderm formation in Xenopus ectodermal explants overexpressing Xwnt8: evidence for a cooperating signal reaching animal pole by gastrulation. Development **118:**1335–1342.
54. **Symes, K., and J. C. Smith.** 1987. Gastrulation movements provide an early marker of mesoderm induction in Xenopus laevis. Development **101:**339–349.
55. **Tang, T. L., R. M. Freeman, A. M. O'Reilly, B. G. Neel, and S. Y. Sokol.** 1995. The SH2-containing protein tyrosine phosphatase SH-PTP2 is required upstream of MAP kinase for early Xenopus development. Cell **80:**473–483.
56. **Tapon, N., and A. Hall.** 1997. Rho, Rac, and Cdc42 GTPases regulate the organization of the actin cytoskeleton. Curr. Opin. Cell Biol. **9:**86–92.
57. **Timms, J. F., K. Carlberg, H. Gu, H. Chen, S. Kamatkar, L. R. Rohrschneider, and B. G. Neel.** 1998. Identification of major binding proteins and substrates for the SH2-containing protein tyrosine phosphatase SHP-1 in macrophages. Mol. Cell. Biol. **18:**3838–3850.
58. **Tsuda, M., T. Matozaki, K. Fukunaga, Y. Fujioka, A. Imamoto, T. Noguchi, T. Takada, T. Yamao, H. Takeda, F. Ochi, T. Yamamoto, and M. Kasuga.** 1998. Integrin-mediated tyrosine phosphorylation of SHPS-1 and its association with SHP-2. J. Biol. Chem. **273:**13223–13229.
59. **Umbhauer, M., C. J. Marshall, C. S. Mason, R. W. Old, and J. C. Smith.** 1995. Mesoderm induction in Xenopus caused by activation of MAP kinase. Nature **376:**58–62.
60. **Van Aelst, L., and C. D'Souza-Schorey.** 1997. Rho GTPases and signaling networks. Genes Dev. **11:**2295–2322.
61. **Van Vactor, D., A. O. O'Reilly, and B. G. Neel.** 1998. Genetic analysis of protein tyrosine phosphatases. Curr. Opin. Gen. Dev. **8:**112–126.
62. **Weidner, K. M., S. Di Cesare, M. Sachs, V. Brinkmann, J. Behrens, and W. Birechmeier.** 1996. Interaction between Gab1 and the c-Met receptor tyrosine kinase is responsible for epithelial morphogenesis. Nature **384:**173–176.
63. **Whitman, M., and D. A. Melton.** 1992. Involvement of $p21^{ras}$ in *Xenopus* mesoderm induction. Nature **357:**252–254.
64. **Yamauchi, K., and J. E. Pessin.** 1995. Epidermal growth factor-induced association of the SHPTP2 protein tyrosine phosphatase with a 115-kDa phosphotyrosine protein. J. Biol. Chem. **270:**14871–14874.
65. **Yu, D.-H., C.-K. Qu, O. Henegariu, X. Lu, and G.-S. Feng.** 1998. Protein-tyrosine phosphatase SHP-2 regulates cell spreading, migration and focal adhesion. J. Biol. Chem. **273:**21125–21131.